

Inductive inference of gradient-boosted decision trees on graphs for insurance fraud detection

Félix Vandervorst^{a,b,c}, Bruno Deprez^{b,c,*}, Wouter Verbeke^b, Tim Verdonck^{c,d}

^a*Allianz Benelux Data Office Koning Albert II Laan 32 Brussels 1000 Belgium*

^b*KU Leuven Faculty of Economics and Business Naamsestraat 69 Leuven 3000 Belgium*

^c*University of Antwerp Department of Mathematics Middelheimlaan 1 Antwerp 2020 Belgium*

^d*KU Leuven Department of Mathematics Celestijnenlaan 200B Leuven 3001 Belgium*

Abstract

Graph-based methods are becoming increasingly popular in machine learning due to their ability to model more complex data and relations. Whereas gradient boosted tree approaches dominate the field of supervised learning on tabular data, (deep) neural network-based approaches are dominantly used for supervised learning on a graph structure. In this paper, inspired by the prime use case of graph learning for fraud detection, we combine gradient boosted trees with structured heterogeneous graph data. We present a novel graph gradient boosting machine (G-GBM) for supervised learning on heterogeneous and dynamic graphs. We show that our estimator competes with popular graph neural network approaches in an experiment using a variety of simulated random graphs. We demonstrate the power of the method for insurance fraud detection using an open-source and a real-world, proprietary dataset. Given that the backbone model is a gradient boosting forest, we apply established explainability methods to gain better insights into the predictions made by G-GBM.

Keywords: Fraud Analytics, Health Insurance, Nonlife Insurance, Heterogeneous Graphs, Machine Learning.

1. Introduction

Insurance fraud costs insurance companies billions every year. This inflated cost is eventually integrated in the premium and hence passed on to the clients. In the United States, the Coalition Against Insurance Fraud estimates that fraud costs more than \$ 300 billion per year ([Coalition Against Insurance Fraud, 2023](#)). The Federal

*Corresponding author: bruno.deprez@kuleuven.be

Bureau of Investigation (FBI) estimates that non-health insurance fraud is worth more than \$40 billion annually (Federal Bureau of Investigation, 2023). In the EU, the European (re)insurance federation estimates that insurance fraud amounts to €13 billion euros yearly and that the total of all cases of fraud—both detected and undetected—amounts to 10% of the total claims expenditure in Europe (Insurance Europe, 2023). In the United Kingdom, the Association of British Insurers reported that in 2021 alone, insurers detected 89,000 dishonest insurance claims valued at £1.1 billion (The Association of British Insurers, 2023).

An effective strategy to detect and prevent fraud is critical for insurance companies to reduce their costs and gain a competitive advantage with a lower insurance premium. Supervised and unsupervised learning methods have been the most popular approaches to (insurance) fraud since the 1990s (Bolton and Hand, 2002). These approaches aim to exploit historical patterns to predict fraudulent cases for further inspection. However, these approaches assume that historical insurance claims are *independent and identically distributed* (i.i.d.).

More recently, graph-based methods have offered new avenues for detecting unexplored patterns and have become a popular method to insurance fraud detection (Óskarsdóttir et al., 2022; Campo and Antonio, 2025; Deprez et al., 2024b). Unlike traditional methods, graph-based methods explicitly model the relationships between individuals, making them appropriate for detecting organized insurance fraud, where multiple parties collaborate to commit fraud (Sadowski and Rathle, 2014).

The effective identification of fraud hubs is of interest, not only for insurance companies, but also for law enforcement agencies, since organised insurance fraud is used to launder money and/or fund further criminal activities.

The complex interaction structure between different parties results in a heterogeneous graph with diverse node and edge types. This heterogeneity is intrinsic to insurance networks, since people and companies, i.e., the clients, interact with the insurer through different policies over their lifetime. Previous network analytics studies often capture this heterogeneity by constructing network embeddings based on metapaths in the network (Sun et al., 2012; Wang et al., 2019; Fu et al., 2020; Cao et al., 2018; Chen et al., 2019) or apply graph neural networks (GNNs) (Deprez et al., 2024b).

Fraud detection involves mostly tabular data with a high class imbalance. Deep learning-based methods, like GNNs, underperform compared to tree-based learning methods (Grinsztajn et al., 2022), like LightGBM (Ke et al., 2017). Moreover, network structures evolve over time, changing a node’s connections, features and even labels. There is thus a need for inductive methods that update the predicted proba-

bility for a node to be fraudulent whenever new information becomes available. This is not possible for many (meta)path-based methods, such as node2vec (Grover and Leskovec, 2016) or metapath2vec (Dong et al., 2017).

To summarise, insurance fraud detection offers a unique and challenging use case, since (1) network information is invaluable, the network structure is inherently (2) heterogeneous and (3) dynamic, and (4) only few cases are ever investigated resulting in a high class imbalance. In this work, we contribute to the state-of-the-art in supervised learning on complex graph structures as applied for, e.g., predict insurance fraud risk. We present a novel method called graph-gradient boosted machine (G-GBM), which combines the detection power of gradient boosting with the complex data representation of heterogeneous networks. It is based on probability-weighted metapaths, which are adapted to gradient-boosted trees. Unlike common GNNs, these metapaths do not require iterative aggregation of local information.

We compare the performance of G-GBN with that of GraphSAGE on simulated random graphs for independent cross-validation, and with that of HinSage on heterogeneous graphs for insurance fraud detection, representing the state-of-the-art in the field. We find that our method outperforms GNNs in both experiments. Additionally, we present an adaptation for G-GBM of the popular SHAP-based explanations in classic supervised learning problems.

Hence, our main contributions are as follows:

- We introduce a new method G-GBM that combines the strength of gradient boosting with the complexity of heterogeneous graph analytics.
- We rigorously test our method against other baselines on a real-world insurance dataset and on open-source and random networks, allowing for reproducibility of our results.
- We make the full implementation of our method publicly available on GitHub: https://github.com/VerbekeLab/GBDT_Graphs.

2. Related work

2.1. Learning on tabular data.

Machine learning methods for fraud detection (including insurance) are essentially dominated by two approaches (Bolton and Hand, 2002; Abdallah et al., 2016): supervised and unsupervised learning (or a combination thereof).

Insurance fraud detection poses different challenges. First, fraud is rare and most insurance claims are never investigated because of resource constraints at insurance

companies. This results in very few labelled cases. Second, fraudsters continuously change tactics, making fraud detection model trained on historical data rapidly obsolete (Van Vlasselaer et al., 2017; Baesens et al., 2015).

Therefore, unsupervised learning has been widely applied for fraud detection, as it does not rely on (historical) labels for training. Unsupervised learning mostly relies on anomaly detection, as fraudulent claims are assumed to be exaggerated or unrealistic, and hence differ substantially from normal claims (Debener et al., 2023; Stripling et al., 2018; Nian et al., 2016; Vandervorst et al., 2022).

Although unsupervised learning seems the obvious choice when dealing with sparsely labelled data, fraud is also imperceptibly concealed (Van Vlasselaer et al., 2017). As a results, not all fraud cases are anomalies and not all anomalies are fraud. Previous research on insurance fraud as well as other types of financial fraud has shown that unsupervised learning often underperforms compared to supervised learning (Debener et al., 2023; Lorenz et al., 2021; Deprez et al., 2024a).

Supervised learning in the context of fraud is typically addressed as a binary classification problem. Historical information on claims and fraud labels, (x_i, y_i) , are assumed to be *independent* realizations of random variables (X_i, Y_i) , following a marginal distribution P_{XY} taking values in $\mathbb{R}^d \times \{0, 1\}$. In fraud detection problems, given that many classification methods are capable of producing continuous output, one generally seeks to determine the posterior distribution $\eta(X) := P(Y = 1|X) = E(Y|X)$ to estimate the probability of fraud based on information x only. The classifier $C : \mathbb{R}^d \rightarrow \{0, 1\}$ can be expressed as (Devroye et al., 2013)

$$C(X) = \begin{cases} 1, & \text{if } \eta(X) \geq \psi. \\ 0, & \text{otherwise.} \end{cases} \quad (1)$$

The threshold ψ is arbitrarily set in a case-dependent manner. Therefore, in the fraud detection literature, one often uses threshold-independent, rank-based performance measures, such as the area under the receiver operating characteristic curve (ROC-AUC) or the area under the precision-recall curve (PR-AUC) to evaluate the performance of a classifier. One strong criteria is (weak) Pareto dominance, where the classifier is superior (or equal) to another for all thresholds. Although it is well known that there is no silver bullet algorithm for learning η in Equation (1) for all possible distributions of P_{XY} (Devroye et al., 2013), some algorithms seem generally more powerfull and are more commonly used in practice than others. Popular state-of-the-art methods in machine learning are gradient-boosted tree methods, such as LightGBM (Ke et al., 2017), XGBoost (Chen and Guestrin, 2016), and CatBoost (Prokhorenkova et al., 2018). These models are often showcased in experiments to

be superior to neural networks (deep learning) on tabular datasets (Shwartz-Ziv and Armon, 2022; Grinsztajn et al., 2022).

2.2. Supervised learning with graph features.

More recently, graph learning methods have gained traction in the field of fraud detection. Graphs can be used to represent the relationships between individuals or entities. Such information has been shown to be useful for detecting organized insurance fraud (Sadowski and Rathle, 2014). A common approach to learn from graphs involves enriching the classical supervised learning problem with new features that are generated from the graph structure (X'_i, Y_i) , where the new vector $X'_i := X_i \parallel X_i^G$ is the concatenation of the “intrinsic” (node) features X_i and graph-based features X_i^G (Óskarsdóttir et al., 2022; Deprez et al., 2024b). These new graph features can be based on simple graph statistics (e.g., degree and betweenness), guilt by association features (e.g., PageRank (Page et al., 1999)), random walk-based features (e.g., DeepWalk (Perozzi et al., 2014) and Node2Vec (Grover and Leskovec, 2016)) or neural network-based features (e.g., graph convolutional networks (Kipf and Welling, 2016) and GraphSAGE (Hamilton et al., 2017a)). In the context of (insurance) fraud, “guilt by association” has been proven to be particularly effective (Šubelj et al., 2011; Óskarsdóttir et al., 2022; Menon, 2018; Van Vlasselaer et al., 2017; Deprez et al., 2024b), where the estimator of fraud probability $P(Y_i = 1|Y_{j \neq i}, \mathcal{G}(\mathcal{V}, \mathcal{E}))$ is from the joint distribution $P(Y_1, \dots, Y_n|\mathcal{G}(\mathcal{V}, \mathcal{E}))$, and $\mathcal{G}(\mathcal{V}, \mathcal{E})$ is a graph structure determining the dependence between random variables Y_1, \dots, Y_n . Calderoni et al. (2020) examined the structure of a criminal network and demonstrated the effectiveness of the Personalized PageRank algorithm. They emphasize the pivotal role of topology selection in graph construction, noting that the choice between using meetings or phone calls as the basis for the graph significantly impacts the results. This finding underscores the critical importance of network design parameters in analysing criminal networks. In the context of detecting motor insurance fraud, Šubelj et al. (2011) presented different possible topologies and highlighted the contrast between utilizing expressive topologies versus simpler representations. In social security fraud, Van Vlasselaer et al. (2017) introduce methods to summarize network characteristics for supervised downstream classification. Cao et al. (2018); Chen et al. (2019) also used “intrinsic” node features supplemented with metapath information (including proximity to other fraud labels) for e-commerce fraud. However, the choice of graph-based features is arbitrary and depends on the application. Recently, graph neural networks have been aimed at generalizing the discovery of graph-based patterns (Deprez et al., 2024b).

2.3. Graph Neural Networks

A recent trend in graph analysis concerns graph network embedding, which aims to condense information from a graph’s neighborhood into a single feature vector. This trend encompasses three distinct methodologies: (i) methods based on matrix factorization, (ii) techniques based on random walks, such as DeepWalk (Perozzi et al., 2014) and Node2Vec (Grover and Leskovec, 2016), and (iii) more recent approaches utilizing graph neural networks (GNNs), such as GraphSAGE (Hamilton et al., 2017a).

In the supervised learning context, GNNs take advantage of more information (e.g., node attributes) to learn the conditional distribution $P(Y_i = 1 | \mathcal{G}(\mathcal{V}, \mathcal{E}, \psi))$, where ψ is a mapping function that links nodes \mathcal{V} to their corresponding random variables X and $\mathcal{G}(\mathcal{V}, \mathcal{E}, \psi)$ is called an *attributed* graph. GNNs learn these conditional distributions by iteratively aggregating neighbourhood information, based on message passing.

When learning on heterogeneous graphs, the message passing is split and learned according to the relation type (Schlichtkrull et al., 2018). Since not all relation types are as meaningful, Wang et al. (2019) introduced semantic-level attention to their heterogeneous graph attention network (HAN). Van Belle et al. (2022, 2023) used graph network embedding for credit card fraud prediction, particularly HinSage, a heterogeneous graph extension of the popular GraphSAGE (Hamilton et al., 2017b) method. This has been extended by Van Belle and De Weerdt (2024) to be better suited to deal with skewed class distributions.

A common assumption in supervised learning on graphs is that the influence of distant nodes fades as the distance increases. In other words, $\exists k : \forall d(v, u) > k, (X_v, Y_v) \perp\!\!\!\perp (X_u, Y_u)$, where $d(u, v)$ is the geodesic distance (or the shortest path distance) between nodes u and v . This assumption motivates us to formulate supervised learning on attributed graphs by establishing a subgraph \mathcal{G}_v^n , the local neighborhood of size n centered in node v . Equation (1) becomes:

$$C(\mathcal{G}_v^n) = \begin{cases} 1, & \text{if } \eta(\mathcal{G}_v^n) \geq \psi. \\ 0, & \text{otherwise.} \end{cases} \quad (2)$$

Beyond applications in fraud detection, there is considerable ongoing research in graph-based machine learning that focuses on more complex and expressive forms of graphs, including those that are heterogeneous and time dependent. As an extensive discussion on graph neural networks (GNNs) is beyond the scope of this paper, we refer to Shi et al. (2022) for a recent comprehensive overview of GNNs.

As noted in Hamilton et al. (2017b), there is much work to do to improve the theoretical framework to guide future graph-based methods. In particular, in the

field of heterogeneous graph neural networks, a theoretical framework is lacking (Shi et al., 2022). Much work is also needed to improve the reliability of graph learning and its interpretability, which is particularly important for fraud applications, and to address methodological concerns of dependence between training and testing on overlapping graphs, a problem often ignored in graph research.

2.4. Random Graphs

One particular field of research that studies the theoretical properties of graphs is random graph theory. It examines the graph-generating process $P(\mathcal{G})$, its properties and relevance for explaining empirically observed (social) networks. In turn, those graphs can be used to simulate *independent* graphs for a more accurate comparison of algorithms (e.g., by generating independent training and test graphs). Erdős-Rényi (Erdős and Rényi, 1959) is the first and simplest random graph model in which nodes are randomly connected with a probability p independent of other edges. The stochastic block model (SBM) (Holland et al., 1983) extends random graphs to include the community structure, with edges placed randomly based on predefined groups or blocks, which can represent, for example, communities. The Watts-Strogatz model (Watts and Strogatz, 1998) creates small-world networks by rewiring the edges of a regular lattice with probability p and interpolating between regular and random graphs. Kleinberg (2000) generalizes the Watts-Strogatz model with long-range contacts to a grid-like network with the probability of long-range connections decreasing as a power-law function of distance. The Barabási-Albert (BA) model (Barabási and Albert, 1999) is the first random graph with the “scale-free” property which is widely observed empirically in social networks, preferentially attaching new nodes to those with higher degrees. Bianconi and Barabási (2001) extended the BA model by incorporating a fitness parameter in each node, allowing “late joiners” to gain an edge over the first mover. To our knowledge, the literature on more elaborate forms of random graphs is fairly limited. Pfeiffer III et al. (2014) presents an attributed graph model (AGM) that models correlations among features and possibly learns those correlations in an existing (homogeneous) network.

Recently, simulated network data was introduced for insurance fraud detection. Campo and Antonio (2025) built an engine consisting of seven steps to simulate networks of claims and involved parties. Each step is based on insights from previous research to keep the simulations comprehensible yet realistic.

3. Methodology

In this section, we discuss elements from graph learning to introduce our novel method: G-GBM. First, we define heterogeneous information networks (HINs). Sec-

ond, we define simple path representations of egonets and representations of node and edge features along those paths. Third, we present our G-GBM method, which elegantly uses probability-weighted featurised paths to exploit the information from the node and edge features. A formal description of G-GBM in pseudo-code is provided as Algorithm 1.

Algorithm 1 G-GBM

Input: Network $\mathcal{G}(V, E, \phi, \psi, \chi, \xi)$, metapath schema \mathcal{P}

Output: Predictions $\hat{\eta}(\mathcal{G}_v^n)$ for node v and its egonet \mathcal{G} of size n .

- 1: Sample all metapaths according to \mathcal{P} starting at v
- 2: **for** metapaths p **do**
- 3: Calculate weights $\mathcal{P}(P_{v,p}^n)$ according to Equation (3)
- 4: Calculate features $x_{v,p}^n$ according to Equations (4)-(6)
- 5: **end for**
- 6: Train gradient boosting forest $\hat{\eta}_v^p(x_{v,p}^n)$
- 7: $\hat{\eta}(\mathcal{G}_v^n) = \sum_p \mathcal{P}(P_{v,p}^n) \hat{\eta}_v^p(x_{v,p}^n)$

3.1. Heterogeneous Information Networks.

A graph containing multiple types of nodes and/or edges is called a **heterogeneous information network (HIN)**, denoted as $\mathcal{G}(\mathcal{V}, \mathcal{E}, \phi, \psi, \chi, \xi)$, where

- \mathcal{V} is the set of nodes.
- \mathcal{E} is the set of edges; $\mathcal{E} \subset \mathcal{V} \times \mathcal{V}$.
- $\phi : \mathcal{V} \rightarrow \mathcal{T}$ is the node type mapping function, with $\phi(v) \in \mathcal{T}, \forall v \in \mathcal{V}$, indicating the unique node type for node every v .
- $\psi : \mathcal{E} \rightarrow \mathcal{R}$ is the edge relation type mapping function, with $\psi(e) \in \mathcal{R}, \forall e \in \mathcal{E}$, indicating the unique relation type for every edge e .
- $\chi : \mathcal{V} \rightarrow \bigcup_{\tau \in \mathcal{T}} \mathbb{R}^{d_\tau}$ is the node feature mapping function, where each node v is assigned to a feature vector in space \mathbb{R}^{d_τ} . Dimension d_τ corresponds to node type $\tau = \phi(v)$, allowing the dimension to vary depending on the node type.
- $\xi : \mathcal{E} \rightarrow \bigcup_{\rho \in \mathcal{R}} \mathbb{R}^{f_\rho}$ is the edge feature mapping function, where each edge e is mapped to a feature vector in a space \mathbb{R}^{f_ρ} . Dimension f_ρ corresponds to edge type $\rho = \psi(e)$, allowing the dimension vary depending on the edge type.

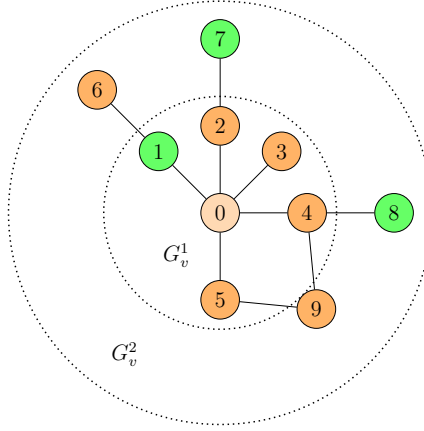


Figure 1: An ego-net G_v^n of size $n=2$ centered on node v with two node types: companies (orange) and administrators (green). The simple path set $P(v)^n$ (edges are omitted for compactness) is: $\{(v_0, v_1, v_6), (v_0, v_2, v_7), (v_0, v_3), (v_0, v_4, v_8), (v_0, v_4, v_9), (v_0, v_5, v_9)\}$

$|\mathcal{T}|$ and $|\mathcal{R}|$ are the numbers of node and edge types, respectively. A graph having only one type of node and edge is called a **homogeneous network**, i.e., $|\mathcal{T}| = 1$ and $|\mathcal{R}| = 1$.

3.2. Local graph information: Ego-net and metapaths.

Let N_v^k be the set of nodes that are exactly k steps away from v for a node v in graph \mathcal{G} :

The **ego-net** \mathcal{G}_v^n of the vertex v , as presented in Figure 1, is the induced subgraph of \mathcal{G} with the vertex set $\mathcal{V}_v^n = \{v\} \cup \bigcup_{k=1}^n N_v^k$ and the edge set $\mathcal{E}_v^n \subseteq \mathcal{E}$, where $(u, w) \in \mathcal{E}_v^n$ if and only if $(u, w) \in \mathcal{E}$ and both u and w are in \mathcal{V}_v^n :

$$\begin{aligned} \mathcal{V}_v^n &= \{v\} \cup \bigcup_{k=1}^n N_v^k, \\ \mathcal{E}_v^n &= \{(u, w) \in \mathcal{E} \mid u, w \in \mathcal{V}_v^n\}. \end{aligned}$$

In a heterogeneous graph \mathcal{G} , a **simple path** of length k from a node v to a node v_k is a sequence of nodes and edges $(v_0 = v, e_1, v_1, e_2, \dots, e_k, v_k)$ such that

- For each i ($1 \leq i \leq k$), $e_i = (v_{i-1}, v_i) \in \mathcal{E}$, each pair of consecutive nodes in the path is connected by an edge in the graph.
- All nodes in the sequence are distinct: for any $0 \leq i, j \leq k$, $i \neq j$, $v_i \neq v_j$.

We define the **set of simple paths** in ego-net \mathcal{G}_v^n as: $P(v)^n = \{P \mid P \text{ is an } v\text{-path of length } \leq n \text{ in } \mathcal{G}_v^n\}$

The types of nodes and edges can vary in a simple path, reflecting the heterogeneous nature of the graph. Each node v_i can be of any type $\phi(v_i) \in \mathcal{T}$ and each edge e_i can be of any type $\psi(e_i) \in \mathcal{R}$. Alternatively, it is common to use a **metapath**, which is defined as a specific sequence of node and edge types.

The definition of metapaths has the advantage of explicitly representing only possible paths, which can facilitate computations when this information is available. The available information is approximated based on probable featurised path aggregation using metapaths.

Each path is assigned a relative weight, used as case weights in the down-stream decision tree algorithm. Let us denote the probability of a random walker taking a path from v to p by $\mathcal{P}(P_{v,p}^n)$, and then naturally, $\sum_p \mathcal{P}(P_{v,p}^n) = 1$. Then, $\mathcal{P}((v_0, e_1, v_1, \dots e_k, v_k))$ is defined as:

$$\mathcal{P}((v_0, e_1, v_1, \dots e_k, v_k)) := \prod_{i=1}^k p(v_{i-1}, e_i, v_i | \mathcal{G}^{(i)}), \quad (3)$$

where $\mathcal{G}^{(i)} := \mathcal{G}^{(i-1)} \setminus \{v_{i-1}, e_i\}$ for $i > 0$ and $\mathcal{G}^{(0)} = \mathcal{G}$ is the subgraph of \mathcal{G} excluding the entries visited at step (i) in the simple path.

3.3. Ego-net paths to supervised learning.

The representation of node and edge attributes along a given simple path is defined as follows. We define the n -length featurization function $h : P \rightarrow \{R, \emptyset\}^{n \times (\sum_{i \in \mathcal{T}} d_i + \sum_{j \in \mathcal{R}} d_j)}$ of path $P_{v,p}^n$ as

$$\begin{aligned} h(P_{v,p}^n) &:= \left(\left\| \chi_i(v_0) \right\|_{i \in \mathcal{T}} \right) \left\| \left[\left\| \left(\left(\left\| \xi_j(\{v_{k-1}, v_k\}) \right\|_{j \in \mathcal{R}} \right) \left\| \left(\left\| \chi_i(v_k) \right\|_{i \in \mathcal{T}} \right) \right) \right] \right\| \\ &:= x_{v,p}^n \end{aligned} \quad (4)$$

where $(v_0, \dots, v_{n'})$ is the order sequence of vertices in $P_{v,p}^n$. We note that $n' \leq n$ allows for early stopping, in case the path arrives at a dead end. The functions χ_i, ξ_j assign

the feature values:

$$\chi_i(v_k) = \begin{cases} \chi(v_k) & \text{if } \phi(v_k) = \mathcal{T}^i \text{ and } k < n' \\ \emptyset^{d_i} & \text{otherwise} \end{cases}, \quad (5)$$

$$\xi_j(\{v_{k-1}, v_k\}) = \begin{cases} \xi(\{v_{k-1}, v_k\}) & \text{if } \psi(\{v_{k-1}, v_k\}) = \mathcal{R}^j \text{ and } k < n' \\ \emptyset^{d_j} & \text{otherwise} \end{cases}, \quad (6)$$

where $k > n'$ expresses that the path is shorter than the maximal length.

Note that the above definition can be simplified for specific graph topologies. For instance, an HIN with multiple node types and features but only one type of edge, with no edge features, simplifies to

$$h(P_{v,p}^n) := \prod_{k=0}^n \left(\prod_{i \in \mathcal{T}} \chi_i(v_k) \right). \quad (7)$$

Ultimately, we are interested in classifying a node as fraudulent or non-fraudulent, based on these featurised path vectors. The loss function of the problem is written as $\mathcal{L}(y_v, \hat{y}_v)$ for any node v . Our proposed method is an estimator of $\eta(\mathcal{G}_v^n)$ from Equation (2) based on its metapath predictions weighted by their random walk probabilities, as follows:

$$\hat{\eta}(\mathcal{G}_v^n) = \sum_p \mathcal{P}(P_{v,p}^n) \hat{\eta}_v^p(x_{v,p}^n) \quad (8)$$

where $\hat{\eta}^p := \hat{\mathcal{P}}(y_{v,p} = 1 | x_{v,p}^n)$. In other words, the probability of fraud of a given node v with respect to its local neighborhood G_v^n is the sum of their estimated probability of path fraud, weighted by the probability of a random walker taking this path. Equation (8) can be interpreted as a weighted loss function.

We also note the case of either an ego-net of size null or a fully disconnected graph (i.e., with no edges). For a supervised learning task where the head node is of one specified type, our estimator reverts to the classical supervised learning problem of Equation (1). Indeed, each node presents only one simple path (itself), so $|p| = 1$, $\mathcal{P}(P_{v,p}^n) = 1$, $x_{v,p}^n$ refers to samples x_i , and our estimator of Equation (8) is the typical supervised learning estimator of Equation (1).

The fraud probabilities of G-GBM are determined using an adaptation of gradient boosted decision trees, with case weights to estimate $\hat{\eta}_v$. In decision tree algorithms, the Gini impurity measures how often a randomly chosen element from the set would be incorrectly labeled if it were randomly labeled according to the distribution of

labels in the subset. It is used as a split criterion in constructing a decision tree. For a set S containing samples of various classes, the Gini impurity is calculated as:

$$\text{Gini}(S) = 1 - \sum_{i=1}^{|\mathcal{Y}|} (\Delta_i)^2, \quad (9)$$

where $|\mathcal{Y}|$ is the number of classes and Δ_i is the proportion of samples in S that belong to class i .

In the context of sample weights, the proportion Δ_i is computed by summing the weights (hence, the probability of their paths) of the samples in each class instead. The weighted Gini impurity for a set S is:

$$\text{Gini}_w(S) = 1 - \sum_{i=1}^{|\mathcal{Y}|} \left(\frac{\sum_{x_{v,p}^n \in S_i} \mathcal{P}(P_{v,p}^n)}{\sum_{x_{v,p}^n \in S} \mathcal{P}(P_{v,p}^n)} \right)^2, \quad (10)$$

where S_i is the subset of S that belongs to class i , and $\mathcal{P}(P_{v,p}^n)$ is the weight of the sample $x_{v,p}^n$.

When considering a split of S into two subsets S_L and S_R , the weighted Gini impurity for the split is a weighted average of the impurities of the two subsets:

$$\begin{aligned} \text{Gini}_{\text{split}}(S_L, S_R) &= \frac{\sum_{x_{v,p}^n \in S_L} \mathcal{P}(P_{v,p}^n)}{\sum_{x_{v,p}^n \in S} \mathcal{P}(P_{v,p}^n)} \text{Gini}_w(S_L) \\ &+ \frac{\sum_{x_{v,p}^n \in S_R} \mathcal{P}(P_{v,p}^n)}{\sum_{x_{v,p}^n \in S} \mathcal{P}(P_{v,p}^n)} \text{Gini}_w(S_R) \end{aligned} \quad (11)$$

The algorithm will choose the split that results in the lowest weighted Gini impurity, which implies the greatest increase in the “purity” of the resulting subsets, taking into account the case weights.

Furthermore, our method can generate missing values (denoted by \emptyset in the above). The Gini criterion is adapted as follows: consider $S'_L := (S_L \cup S)$ and $S'_R := (S_R \cup S)$.

$$\text{Gini}'_{\text{split}} = \text{argmax} (\text{Gini}_{\text{split}}(S'_L, S_R), \text{Gini}_{\text{split}}(S_L, S'_R)) \quad (12)$$

In LightGBM (Ke et al., 2017), XGBoost (Chen and Guestrin, 2016), CatBoost (Prokhorenkova et al., 2018) and other gradient boosting frameworks that support case weights, this concept is applied during the construction of trees. Since $\sum_p \mathcal{P}(P_{v,p}^n) = 1$ and all the featurised paths of node v belong to the same class as its head node, Equation (10) is equivalent to Equation (9). Therefore, considering only

splits over the features of its head nodes, our algorithm is equivalent to the typical supervised learning algorithm. However, our method has the advantage of using further splits from neighborhood observations. Therefore, our method G-GBM should perform at least as well as its classic supervised counterpart GBM if the implemented model is not sensitive to the (potentially irrelevant) additional dimensions added by the featurised paths.

4. Experiments

The first part of the experiments consists of a simulation study to illustrate the general usability of the proposed method. We compare our method to GraphSAGE on simulated random (homogeneous) graphs. The use of random graphs enables us to control the independence of the training and testing sets.

We present an application to insurance fraud detection on two heterogeneous graph. The first is a real-world, proprietary insurance graph, where we showcase the “out-of-time” prediction capabilities of G-GBM. The second is an open-source graph on health-care provider fraud. With the inclusion of open-source data, we aim for strong reproducibility of our results.

4.1. *Simulation study*

We compare our (inductive) method based on boosted decision trees to GraphSAGE ([Hamilton et al., 2017a](#)), a popular inductive graph neural network method. We use simulated datasets to control the environments and gain insight into the situations where our method performs better and when it does not. We consider popular random graph models in social networks, as introduced in Section [2.4](#), which present archetypal properties observed empirically, such as clustering and degree distribution.

We consider a simple i.i.d. setup of the attributes x_i to explore different possible dependence structures between fraud and its local neighborhood features. In particular, a popular approach to fraud detection is anomaly detection. Therefore, for this simulation study, we consider different situations where “abnormal” feature values closely connected to a node are indicative of fraud.

We consider two scenarios; average neighborhood likelihood and path-dependent likelihood.

4.1.1. Scenario 1: average neighborhood likelihood

In this scenario, each node v has a score s from the likelihoods of its neighborhood features x_i :

$$s(v) = \frac{1}{|G_v^n|} \sum_{v_i \in G_v^n} l(x_i)$$

where $|G_v^n|$ is the number of nodes in G_v^n and the likelihood with respect to a normal $\mathcal{N}(0, 1)$ is $l(x_i) := \frac{1}{\sqrt{2\pi}} e^{-\frac{x_i^2}{2}}$. The simulated fraud labels are assigned as follows:

$$y = \begin{cases} 1, & \text{if } s(v) < \alpha, \\ 0, & \text{otherwise,} \end{cases} \quad (13)$$

where α is set so that ten percent of the cases are classified as fraud (based on expert consensus on the expected proportion of fraud) in the score set $\{s(v_1), \dots, s(v_n)\}$.

4.1.2. Scenario 2: path-dependent likelihood

In the second scenario, we consider a subtler pattern.

$$s(v) = \frac{1}{|p|} \sum_{p \in P_{v,p}^n} \text{Agg}(\{l(x_i)\}_p)$$

where $\{l(x_i)\}_p$ is the set of likelihoods along the path p and Agg is an aggregation function, e.g., Min, Max, Mean.

This expression gives us the likelihood of x_i , assuming it follows a standard normal distribution $\mathcal{N}(0, 1)$. If x_i is a sample from a normal distribution with mean μ and standard deviation σ , we can adjust the likelihood calculation accordingly.

Figure 2 shows the approach for the different random graphs that are considered. Table 1 and Table 2 present the average and standard deviation of the area under the curve (AUC) for 20 (independent) runs for scenario 1 & 2, respectively. During each run, a new graph of 200 nodes is independently drawn for training, validation, and testing. By generating independent graphs using the random graph methods discussed before, we can prevent information spillovers between training, validation, and testing for more robust conclusions. We see that our method is competitive with GraphSAGE in scenario 1 and outperforms GraphSAGE in scenario 2.

4.2. Proprietary Dataset

The real-world dataset contains information on companies in Belgium and concerns the relationships between companies and administrators who work for one or

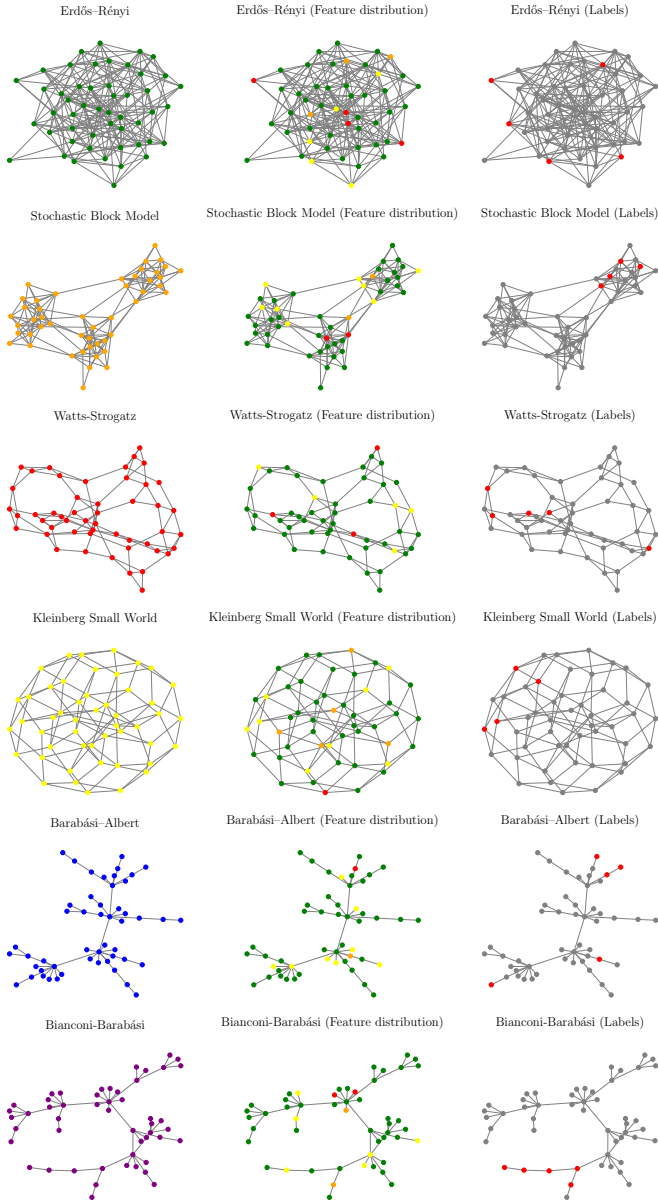


Figure 2: Different random graph model examples with 50 nodes. The features x_i presented in the middle column are univariate and i.i.d. (independently and identically distributed), following a distribution $\mathcal{N}(0, 1)$. The colors (red, orange, yellow) indicate quantiles of the distribution: 5%, 10%, and 20%, respectively, to represent “abnormal” values. The right-hand column presents the labels y_i , which are the top 10% nodes whose 2-hop neighborhood average likelihood is the lowest (hence, y_i are **not** independent).

Table 1: Comparison of GraphSAGE and G-GBM across Different Graph Models

Graph	GraphSAGE	G-GBM	P-Value	T-Statistic
Barabási-Albert	0.662 ± 0.146	0.698 ± 0.096	0.360 276	-0.93
Bianconi-Barabási	0.770 ± 0.088	0.715 ± 0.107	0.086 008	1.76
Erdős-Rényi	0.826 ± 0.078	0.943 ± 0.058	0.000 005	-5.40
Kleinberg Small World	0.539 ± 0.084	0.511 ± 0.069	0.257 902	1.15
Stochastic Block Model	0.846 ± 0.095	0.940 ± 0.054	0.000 541	-3.87
Watts-Strogatz	0.716 ± 0.112	0.775 ± 0.089	0.072 684	-1.85

Table 2: Performance Comparison of GraphSAGE and G-GBM on Various Graph Models Across Different Path Aggregation Modes (Mode)

Graph	Mode	GraphSAGE	G-GBM	P-Value	T-Statistic
Barabási-Albert	Mean	0.888 ± 0.037	0.922 ± 0.036	5.83×10^{-3}	-2.92
Bianconi-Barabási	Mean	0.892 ± 0.055	0.931 ± 0.024	7.04×10^{-3}	-2.93
Erdős-Rényi	Mean	0.920 ± 0.037	0.918 ± 0.034	0.87	0.17
Kleinberg Small World	Mean	0.929 ± 0.035	0.952 ± 0.022	1.88×10^{-2}	-2.48
Stochastic Block Model	Mean	0.869 ± 0.065	0.930 ± 0.027	6.51×10^{-4}	-3.89
Watts-Strogatz	Mean	0.870 ± 0.051	0.917 ± 0.015	7.72×10^{-4}	-3.89
Barabási-Albert	Max	0.755 ± 0.058	0.869 ± 0.029	1.48×10^{-8}	-7.89
Bianconi-Barabási	Max	0.762 ± 0.043	0.864 ± 0.023	3.45×10^{-10}	-9.34
Erdős-Rényi	Max	0.778 ± 0.058	0.852 ± 0.029	1.98×10^{-5}	-5.12
Kleinberg Small World	Max	0.783 ± 0.048	0.822 ± 0.048	1.61×10^{-2}	-2.52
Stochastic Block Model	Max	0.757 ± 0.057	0.869 ± 0.030	1.62×10^{-8}	-7.75
Watts-Strogatz	Max	0.723 ± 0.068	0.877 ± 0.031	1.06×10^{-9}	-9.17
Barabási-Albert	Min	0.908 ± 0.046	0.934 ± 0.040	0.061	-1.93
Bianconi-Barabási	Min	0.905 ± 0.042	0.945 ± 0.043	0.0059	-2.92
Erdős-Rényi	Min	0.914 ± 0.048	0.947 ± 0.040	0.024	-2.35
Kleinberg Small World	Min	0.928 ± 0.095	0.975 ± 0.037	0.052	-2.04
Stochastic Block Model	Min	0.884 ± 0.042	0.936 ± 0.032	0.000 11	-4.35
Watts-Strogatz	Min	0.913 ± 0.046	0.954 ± 0.032	0.0020	-3.34

multiple companies. The dataset contains attributes on companies, e.g., the legal form of the company, the geographical district, the number of workers, and attributes of administrators, e.g., age category and gender.

The observations contain a fraud label if they have committed fraud on any of their policies. This includes a wide range of possible cases. A fraud case could be data misrepresentation in underwriting fraud or the reporting of fake claims or any

other kind.

Unlike in the simulation setup of Section 4.1 where the graphs used for training, validation and testing are independent, this only consider a single graph. To ensure the experimental setup resembles a realistic situation, we distinguish between two time periods:

- Information available at time t_0 , i.e., a graph of companies and administrators captured at that point in time and the fraud labels collected historically up to that point in time.
- Information available at time t_1 , i.e., an updated graph of companies and administrators (which can have newly added or deleted elements compared to t_0) and the fraud labels discovered between t_0 and t_1 .

Table 3 shows the basic characteristics of the graphs \mathcal{G}_{t_0} , \mathcal{G}_{t_1} . We also present their intersection graph $\mathcal{G}_{t_0} \cap \mathcal{G}_{t_1}$ to highlight the persistent nodes and edges and determine the pace at which the network evolves over the period.

Table 3: Real-world dataset: Two graphs \mathcal{G}_{t_0} and \mathcal{G}_{t_1} and their intersection $\mathcal{G}_{t_0} \cap \mathcal{G}_{t_1}$

	\mathcal{G}_{t_0}	\mathcal{G}_{t_1}	$\mathcal{G}_{t_0} \cap \mathcal{G}_{t_1}$
Number of Nodes	2.9e+6	3.1e+6	2.7e+6
- Company	1.5e+06	1.6e+6	1.3e+06
- Admin.	1.4e+06	1.6e+6	1.4e+06
Number of Edges	1.98e+6	2.2e+6	1.9e+6
- Company-Company	9.8e+4	10.8e+4	8.5e+4
- Company-Admin.	1.9e+6	2.2e+6	1.8e+6
Average Degree	1.37	1.42	1.42
- Company	1.40	1.49	1.51
- Admin.	1.34	1.34	1.33

We observe that company-to-company relationships are relatively scarce compared to company-to-administrator relationships but show a proportional increase in the latter time frame, as indicated by the increasing numbers from \mathcal{G}_{t_0} to \mathcal{G}_{t_1} . The persistence of company-to-administrator edges in the intersection graph shows that those edges are relatively stable over the period.

The distribution of labels in each set is presented in Table 4. The labels are collected in two time periods of equal length and contain positive and negative samples.

Table 4: Labels per node type for the proprietary insurance dataset.

Time window	Node type	Labels	Class balance
$]t_{-1}, t_0]$	Admin	7k	22%
$]t_0, t_1]$	Admin	6k	27%
$]t_{-1}, t_0]$	Company	11k	49%
$]t_0, t_1]$	Company	9k	53%

4.3. Healthcare Provider

We also test G-GBM on an open-source dataset to enhance reproducibility of our results. It contains possible health care provider fraud cases and is available on kaggle¹. This dataset, unfortunately, does not contain ground truth labels of the test set, nor does it contain any time information on the label assignment. For the train-test split, we did a clustering of the nodes using the Louvain methods. These clusters are used for the definition of the split. Using these clusters, we try to avoid data leakage by limiting the metapaths, and hence the feature vectors to stay within the train/test graph.

Table 5 shows the resulting graph characteristics. Table 6 shows the label distribution, indicating a strong class imbalance. As said before, only providers are labelled.

Table 5: Healthcare provider fraud

	G_0	G_1
Number of Nodes	81,855	62,042
- Beneficiary	79,255	59,261
- Provider	2600	2781
Number of Edges	205,386	146,205
- Provider-Beneficiary	205,386	146,205
Average Degree	5.02	4.71
- Beneficiary	2.59	2.47
- Provider	78.99	52.57

Our method requires all nodes to have features, however, HCP dataset does not provide any features for the (labelled) provider nodes. Therefore, we construct four features based on the claims data for each provider. These are (1) the number of

¹<https://www.kaggle.com/datasets/rohitrox/healthcare-provider-fraud-detection-analysis>

Table 6: Labels for the health care provider dataset.

Graph	Node type	Labels	Class balance
G_0	Provider	278	11%
G_1	Provider	228	8%

claims, the (2) average and (3) standard deviation of the amount paid, and (4) the number of beneficiaries. We used the provided features for the beneficiary nodes.

4.4. Baseline Methods

Our proposed G-GBM method is tested against a couple of relevant baselines. First, given that G-GBM combines LightGBM with metapaths, we compare it to LightGBM (Ke et al., 2017) that trained on only the node features. Second, Node embeddings coming from metapath2vec (Dong et al., 2017) are used to analyse the impact of the network structure on the predictions. These node embeddings are once used on their own to make predictions and once in combination with the node features. The downstream classifier is again a LightGBM model. Third, we compare G-GBM to HINsage, a GNN architecture for heterogeneous graphs based on GraphSAGE (Hamilton et al., 2017a). HINsage directly incorporates the features and network structure to come to a classification model.

We note that metapath2vec is transductive, meaning that we need to construct the network embedding for the full network, containing both train and test data. We will only illustrate its use on the HCP dataset, since the train and test networks are separated. For the proprietary dataset, most of the nodes are shared while labels and edges change, making metapath2vec impractical for this use-case.

4.5. Results

We present the results of our method on our test set on the receiver operating characteristic (ROC) curve. Insights into feature importance are obtained using SHAP values (Lundberg and Lee, 2017). We also extract the (absolute) SHAP value, a common interpretation metric, to highlight the contribution of neighborhood information.

4.5.1. Company node prediction

First, we present the results on companies' labels. We compare our approach, G-GBM, which uses a local neighborhood of size 2, to the baseline GBM, which uses the features of the head node (i.e., the classical supervised learning framework without graph information). This comparison indicates the added value of local neighborhood information. Additionally, we benchmark our method to HinSage as

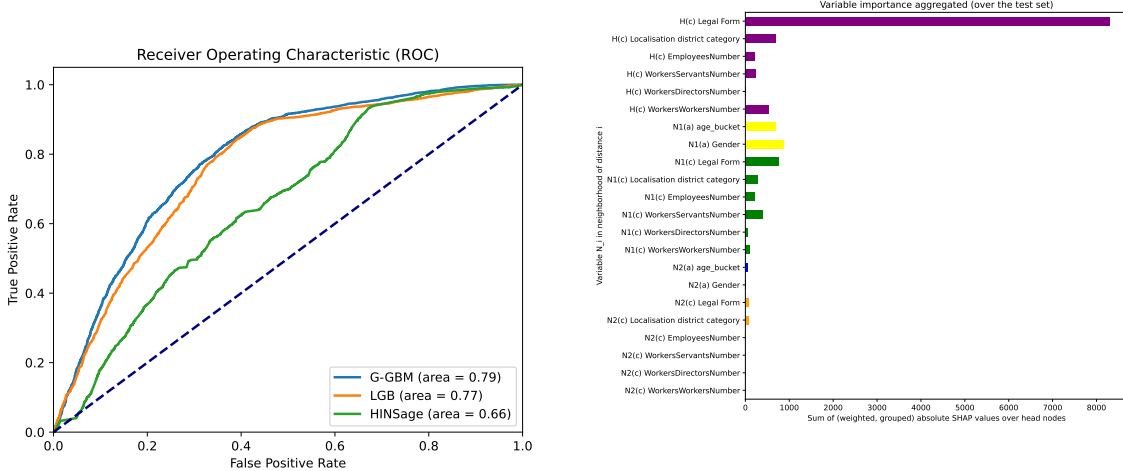


Figure 3: Performance measurements for the test set of company node labels.

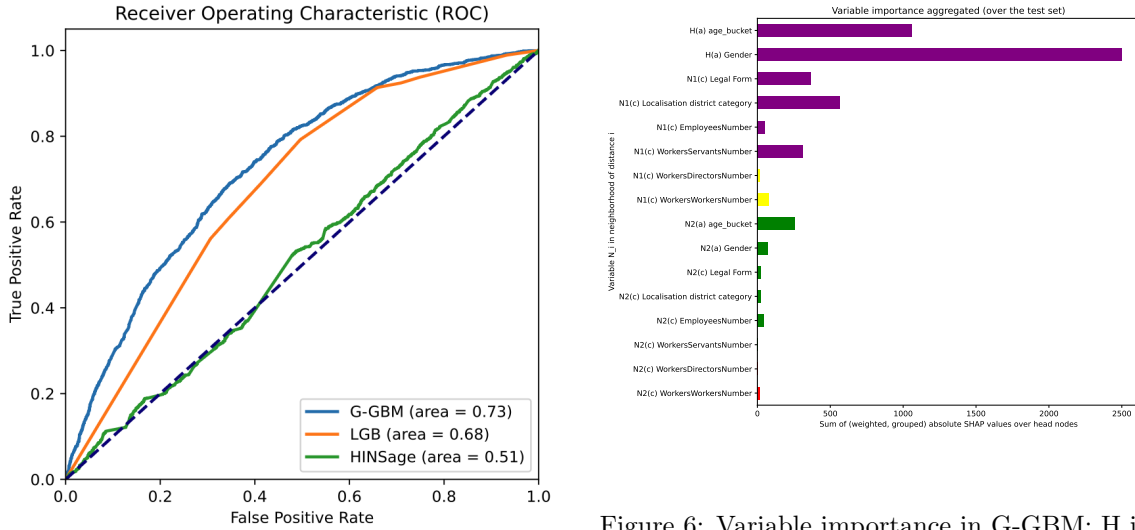
Figure 4: Variable importance in G-GBM: H is the head node, N_q refers to the neighborhood of level q relative to the head node, and (c) and (a) refer to the node type of the company and administrator, respectively.

a challenger GNN approach, which is both inductive and suitable for application on heterogeneous networks.

We first train and test our model on company node labels. The results are presented in Figure 3. We observe that gradient boosting outperforms the GNN model HinSAGE. However, our approach outperforms the baseline methods, with an increase in the ROC-AUC of 0.02 over GBM and 0.13 over HinSAGE.

The increased performance can be attributed to local characteristics, as illustrated by the SHAP values in Figure 4. The SHAP values show that some features of the neighbouring administrator and company contain important information that are leveraged by the fraud detection model.

We observe that G-GBM is Pareto dominant (superior in all segments) compared with both GBM and HinSAGE. The legal form of the company makes the greatest contribution to the G-GBM model prediction. This feature is also available for the baseline GBM model, which explains the models' relatively similar performance. We notice that nodes in the direct neighborhood contribute to the model performance, whereas the second neighborhood level is close to insignificant (which could motivate a reduction in the ego-net size).



4.5.2. Administrator node prediction

Next, we evaluate the prediction of administrator labels using the same procedure. Figure 5 again illustrates the outperformance of gradient boosting over HinSAGE. We observe that G-GBM is Pareto dominant in the GBM and HinSAGE models. The increase in performance achieved by G-GBM is greater than in the previous experiment involving companies. This increase may be explained by the limited information available for head administrator nodes (only an age category and gender information), which limits discrimination power (hence, the piecewise linear appearance of the base GBM approach).

We also notice that the performance of HinSAGE is significantly lower than that of G-GBM in this experiment, with an AUC-ROC value below 0.5. It seems that HinSAGE has difficulties with generalising across the time steps.

The performance difference can be attributed to local characteristics, as shown in Figure 6. Compared to the variable importance attribution in the company case, the contribution is more evenly spread between variables at different neighbourhood levels. The greatest contribution is still coming from the head node.

4.5.3. Healthcare Provider

For the HCP dataset, we only have labels for the providers. Hence, we only have one experiment for this dataset, with no results for the beneficiary nodes. Because

we are working with two separate networks for training and testing, we include experiments based on metapath2vec node embeddings.

The results are provided in Figure 7. We see only a slight improvement of our G-GBM model over the baseline LightGBM and metapath2vec with node features. These models all obtain very high performance, with an AUC-ROC above 90%. HIN-Sage and metapath2vec without additional features, on the other hand, are struggling to find any meaningful embedding.

The similarity between G-GBM, LightGBM and metapath2vec with features can be explained by looking at the variable importance plots in Figure 8. We see that the predictions are mostly done using the features of the head node, meaning that feature information from a node's neighbours does not add meaningful information. The fraud cases can already easily be detected using the four features we constructed in Section 4.3.

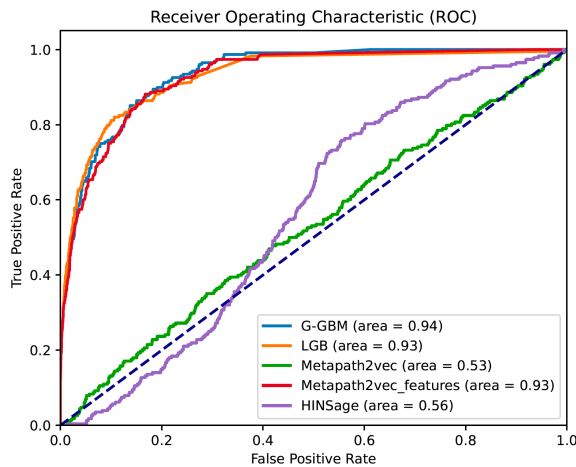


Figure 7: Performance measurement for the test set of HCP provider nodes.

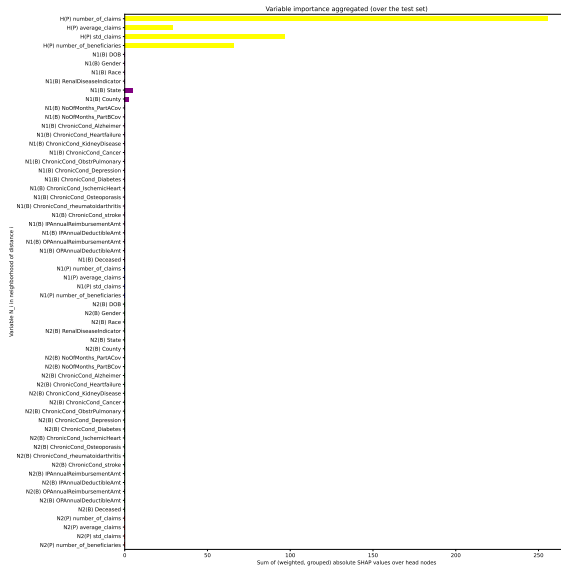


Figure 8: Variable importance in G-GBM: H is the head node, N_q refers to the neighborhood of level q relative to the head node, and (P) and (B) refer to the node type of the provider and beneficiary, respectively.

5. Conclusion

In this paper, we presented G-GBM, a novel method for insurance fraud detection on graphs based on boosted decision trees. These boosted decision trees are shown in the literature to be the dominant method for classification of tabular data. We extended ensembles of gradient boosted trees to graph topologies by concatenating feature vectors alongside simple paths in an egonet and use an elegant adaptation of case weights to construct trees.

We show that our method is consistent with supervised learning methods based only on “intrinsic” features, as it adds only new learnable information from the graph neighbourhood to the classifier, which is experimentally supported by the observed Pareto dominance of G-GBM over GBM in our experiments. The experimental results also show that our method outperforms popular inductive graph supervised learning methods, in a supervised learning setup for fraud detection. However, the purpose of this paper is not to make an exhaustive comparison of all the latest GNN architectures but rather to show that decision trees can also be used and benefit from their desirable properties over GNNs, such as treatment of categorical features, handling of missing data, and explainability. One downside of our method is the expansion of dimensions, which can become computationally impractical in

the case of highly connected networks, many node/edge types, high-dimensional features, or any combination thereof. On the other hand, the method does not require successive aggregation of features, a problem known to lead to over-smoothing in GNN architectures (Li et al., 2018).

Further research could elaborate on random graphs in the context of heterogeneous graphs, as it provides a sounder basis for cross-validation than ignoring the dependence between training and testing sets when using a single graph. In the context of fraud, more specifically, time-aware simple paths enable one to use previous records of fraud as a separate node while controlling for information leakage. Given the popularity of “guilt by association” methods in insurance fraud, we expect this representation to have the potential to reach another performance ceiling. Another promising avenue to improve our method could be the exploration of attention mechanisms, discarding uninformative paths. A possible simplistic extension could be the analysis of SHAP values grouped by meta-path types, thereby discarding irrelevant meta-paths and retraining the model. A more complex attention mechanism (e.g., *there exists at least one path such that...*) would likely require more adaptation than using the case weights, thereby modifying the gradient-boosted model itself.

Acknowledgments

We express our gratitude to Allianz for providing the data that enabled this research.

This work was supported by the Research Foundation – Flanders (FWO research projects 1SHEN24N and G015020N).

References

Abdallah, A., Maarof, M.A., Zainal, A., 2016. Fraud detection system: A survey. *Journal of Network and Computer Applications* 68, 90–113.

Baesens, B., Van Vlasselaer, V., Verbeke, W., 2015. Fraud analytics using descriptive, predictive, and social network techniques: a guide to data science for fraud detection. John Wiley & Sons.

Barabási, A.L., Albert, R., 1999. Emergence of scaling in random networks. *Science* 286, 509–512.

Bianconi, G., Barabási, A.L., 2001. Competition and multiscaling in evolving networks. *Europhysics Letters* 54, 436.

Bolton, R.J., Hand, D.J., 2002. Statistical fraud detection: A review. *Statistical science* 17, 235–255.

Calderoni, F., Catanese, S., De Meo, P., Ficara, A., Fiumara, G., 2020. Robust link prediction in criminal networks: A case study of the sicilian mafia. *Expert Systems with Applications* 161, 113666.

Campo, B.D.C., Antonio, K., 2025. An engine to simulate insurance fraud network data. *European Actuarial Journal* 15, 255–295. URL: <https://doi.org/10.1007/s13385-024-00399-z>, doi:[10.1007/s13385-024-00399-z](https://doi.org/10.1007/s13385-024-00399-z).

Cao, B., Mao, M., Viidu, S., Yu, P., 2018. Collective fraud detection capturing inter-transaction dependency, in: KDD 2017 Workshop on Anomaly Detection in Finance, PMLR. pp. 66–75.

Chen, C., Liang, C., Lin, J., Wang, L., Liu, Z., Yang, X., Zhou, J., Shuang, Y., Qi, Y., 2019. Infdetect: a large scale graph-based fraud detection system for e-commerce insurance, in: 2019 IEEE International Conference on Big Data (Big Data), IEEE. pp. 1765–1773.

Chen, T., Guestrin, C., 2016. Xgboost: A scalable tree boosting system, in: Proceedings of the 22nd ACM SIGKDD international conference on knowledge discovery and data mining, pp. 785–794.

Coalition Against Insurance Fraud, 2023. Coalition Against Insurance Fraud fraud stats. <https://insurancefraud.org/fraud-stats/>. Accessed: 2023-05-05.

Debener, J., Heinke, V., Kriebel, J., 2023. Detecting insurance fraud using supervised and unsupervised machine learning. *Journal of Risk and Insurance* 90, 743–768. URL: <https://onlinelibrary.wiley.com/doi/abs/10.1111/jori.12427>, doi:<https://doi.org/10.1111/jori.12427>.

Deprez, B., Vanderschueren, T., Baesens, B., Verdonck, T., Verbeke, W., 2024a. Network analytics for anti-money laundering – a systematic literature review and experimental evaluation. arXiv preprint arXiv:2405.19383 URL: <https://arxiv.org/abs/2405.19383>, arXiv:2405.19383.

Deprez, B., Vandervorst, F., Verbeke, W., Verdonck, T., Baesens, B., 2024b. Network analytics for insurance fraud detection: a critical case study. *European Actuarial Journal* 14, 965–990. URL: <https://doi.org/10.1007/s13385-024-00384-6>, doi:[10.1007/s13385-024-00384-6](https://doi.org/10.1007/s13385-024-00384-6).

Devroye, L., Györfi, L., Lugosi, G., 2013. A probabilistic theory of pattern recognition. volume 31. Springer Science & Business Media, New York, NY.

Dong, Y., Chawla, N.V., Swami, A., 2017. metapath2vec: Scalable representation learning for heterogeneous networks, in: Proceedings of the 23rd ACM SIGKDD international conference on knowledge discovery and data mining, pp. 135–144.

Erdős, P., Rényi, A., 1959. On random graphs, i. *Publicationes Mathematicae (Debrecen)* 6, 290–297.

Federal Bureau of Investigation, 2023. FBI insurance fraud. <https://www.fbi.gov/stats-services/publications/insurance-fraud>. Accessed: 2023-05-05.

Fu, X., Zhang, J., Meng, Z., King, I., 2020. Magnn: Metapath aggregated graph neural network for heterogeneous graph embedding, in: Proceedings of The Web Conference 2020, Association for Computing Machinery, New York, NY, USA. p. 2331–2341. URL: <https://doi.org/10.1145/3366423.3380297>, doi:10.1145/3366423.3380297.

Grinsztajn, L., Oyallon, E., Varoquaux, G., 2022. Why do tree-based models still outperform deep learning on typical tabular data?, in: Koyejo, S., Mohamed, S., Agarwal, A., Belgrave, D., Cho, K., Oh, A. (Eds.), *Advances in Neural Information Processing Systems*, Curran Associates, Inc.. pp. 507–520. URL: https://proceedings.neurips.cc/paper_files/paper/2022/file/0378c7692da36807bdec87ab043cdadc-Paper-Datasets_and_Benchmarks.pdf.

Grover, A., Leskovec, J., 2016. node2vec: Scalable feature learning for networks, in: Proceedings of the 22nd ACM SIGKDD international conference on Knowledge discovery and data mining, ACM. pp. 855–864.

Hamilton, W., Ying, Z., Leskovec, J., 2017a. Inductive representation learning on large graphs. *Advances in neural information processing systems* 30.

Hamilton, W.L., Ying, R., Leskovec, J., 2017b. Representation learning on graphs: Methods and applications. arXiv preprint arXiv:1709.05584 .

Holland, P.W., Laskey, K.B., Leinhardt, S., 1983. Stochastic blockmodels: First steps. *Social networks* 5, 109–137.

Insurance Europe, 2023. Fraud prevention. <https://www.insuranceeurope.eu/priorities/23/fraud-prevention>. Accessed: 2023-05-05.

Ke, G., Meng, Q., Finley, T., Wang, T., Chen, W., Ma, W., Ye, Q., Liu, T.Y., 2017. Lightgbm: A highly efficient gradient boosting decision tree. *Advances in neural information processing systems* 30.

Kipf, T.N., Welling, M., 2016. Semi-supervised classification with graph convolutional networks. *arXiv preprint arXiv:1609.02907* .

Kleinberg, J., 2000. The small-world phenomenon: An algorithm perspective, in: *Proceedings of the thirty-second annual ACM symposium on Theory of computing*, ACM. pp. 163–170.

Li, Q., Han, Z., Wu, X.m., 2018. Deeper insights into graph convolutional networks for semi-supervised learning. *Proceedings of the AAAI Conference on Artificial Intelligence* 32. doi:[10.1609/aaai.v32i1.11604](https://doi.org/10.1609/aaai.v32i1.11604).

Lorenz, J., Silva, M.I., Aparício, D., Ascensão, J.a.T., Bizarro, P., 2021. Machine learning methods to detect money laundering in the bitcoin blockchain in the presence of label scarcity, in: *Proceedings of the First ACM International Conference on AI in Finance*, Association for Computing Machinery, New York, NY, USA. URL: <https://doi.org/10.1145/3383455.3422549>, doi:[10.1145/3383455.3422549](https://doi.org/10.1145/3383455.3422549).

Lundberg, S.M., Lee, S.I., 2017. A unified approach to interpreting model predictions. *Advances in neural information processing systems* 30.

Menon, N.M., 2018. Information spillover and semi-collaborative networks in insurer fraud detection. *MIS Quarterly* 42, 407–426.

Nian, K., Zhang, H., Tayal, A., Coleman, T., Li, Y., 2016. Auto insurance fraud detection using unsupervised spectral ranking for anomaly. *The Journal of Finance and Data Science* 2, 58–75. URL: <https://www.sciencedirect.com/science/article/pii/S2405918816300058>, doi:<https://doi.org/10.1016/j.jfds.2016.03.001>.

Óskarsdóttir, M., Ahmed, W., Antonio, K., Baesens, B., Dendievel, R., Donas, T., Reynkens, T., 2022. Social network analytics for supervised fraud detection in insurance. *Risk Analysis* 42, 1872–1890.

Page, L., Brin, S., Motwani, R., Winograd, T., 1999. The PageRank citation ranking: Bringing order to the web. Technical Report. Stanford InfoLab.

Perozzi, B., Al-Rfou, R., Skiena, S., 2014. Deepwalk: Online learning of social representations, in: Proceedings of the 20th ACM SIGKDD international conference on Knowledge discovery and data mining, ACM. pp. 701–710.

Pfeiffer III, J.J., Moreno, S., La Fond, T., Neville, J., Gallagher, B., 2014. Attributed graph models: Modeling network structure with correlated attributes, in: Proceedings of the 23rd international conference on World wide web, pp. 831–842.

Prokhorenkova, L., Gusev, G., Vorobev, A., Dorogush, A.V., Gulin, A., 2018. Catboost: unbiased boosting with categorical features. Advances in neural information processing systems 31.

Sadowski, G., Rathle, P., 2014. Fraud detection: Discovering connections with graph databases. White Paper-Neo Technology-Graphs are Everywhere 13.

Schlichtkrull, M., Kipf, T.N., Bloem, P., van den Berg, R., Titov, I., Welling, M., 2018. Modeling relational data with graph convolutional networks, in: Gangemi, A., Navigli, R., Vidal, M.E., Hitzler, P., Troncy, R., Hollink, L., Tordai, A., Alam, M. (Eds.), The Semantic Web, Springer International Publishing, Cham. pp. 593–607.

Shi, C., Wang, X., Philip, S.Y., 2022. Heterogeneous Graph Representation Learning and Applications. Springer.

Shwartz-Ziv, R., Armon, A., 2022. Tabular data: Deep learning is not all you need. Information Fusion 81, 84–90.

Stripling, E., Baesens, B., Chizi, B., vanden Broucke, S., 2018. Isolation-based conditional anomaly detection on mixed-attribute data to uncover workers' compensation fraud. Decision Support Systems 111, 13–26. URL: <https://www.sciencedirect.com/science/article/pii/S016792361830068X>, doi:<https://doi.org/10.1016/j.dss.2018.04.001>.

Šubelj, L., Furlan, Š., Bajec, M., 2011. An expert system for detecting automobile insurance fraud using social network analysis. Expert Systems with Applications 38, 1039–1052.

Sun, Y., Han, J., Aggarwal, C.C., Chawla, N.V., 2012. When will it happen? relationship prediction in heterogeneous information networks, in: Proceedings of the Fifth ACM International Conference on Web Search and Data Mining, Association for Computing Machinery, New York, NY, USA. p. 663–672. URL: <https://doi.org/10.1145/2124295.2124373>, doi:[10.1145/2124295.2124373](https://doi.org/10.1145/2124295.2124373).

The Association of British Insurers, 2023. Fraud. <https://www.abi.org.uk/products-and-issues/topics-and-issues/fraud/>. Accessed: 2023-05-05.

Van Belle, R., Baesens, B., De Weerdt, J., 2023. Catchm: A novel network-based credit card fraud detection method using node representation learning. *Decision Support Systems* 164, 113866.

Van Belle, R., De Weerdt, J., 2024. Shine: A scalable heterogeneous inductive graph neural network for large imbalanced datasets. *IEEE Transactions on Knowledge and Data Engineering* 36, 4904–4915. doi:[10.1109/TKDE.2024.3381240](https://doi.org/10.1109/TKDE.2024.3381240).

Van Belle, R., Van Damme, C., Tytgat, H., De Weerdt, J., 2022. Inductive graph representation learning for fraud detection. *Expert Systems with Applications* 193, 116463.

Van Vlasselaer, V., Eliassi-Rad, T., Akoglu, L., Snoeck, M., Baesens, B., 2017. Gotcha! network-based fraud detection for social security fraud. *Management Science* 63, 3090–3110.

Vandervorst, F., Verbeke, W., Verdonck, T., 2022. Data misrepresentation detection for insurance underwriting fraud prevention. *Decision Support Systems* 159, 113798. URL: <https://www.sciencedirect.com/science/article/pii/S0167923622000690>, doi:<https://doi.org/10.1016/j.dss.2022.113798>.

Wang, X., Ji, H., Shi, C., Wang, B., Ye, Y., Cui, P., Philip, S.Y., 2019. Heterogeneous graph attention network, in: *The World Wide Web Conference*, ACM. pp. 2022–2032. doi:[10.1145/3308558.3313562](https://doi.org/10.1145/3308558.3313562).

Watts, D.J., Strogatz, S.H., 1998. Collective dynamics of ‘small-world’ networks. *Nature* 393, 440–442. URL: <https://doi.org/10.1038/30918>, doi:[10.1038/30918](https://doi.org/10.1038/30918).